Parameterization and testing of a coupled photosynthesis–stomatal conductance model for boreal trees

QING-LAI DANG, [1–3] HANK A. MARGOLIS [1,2,4] and G. JAMES COLLATZ [2]

[1] Centre de Recherche en Biologie Forestière, Faculté de Foresterie et de Géomatique, Université Laval, Sainte-Foy, Québec G1K 7P4, Canada

[2] Biospheric Sciences Branch, Code 923, Building 22, NASA Goddard Space Flight Center, Greenbelt, MD 20771, USA

[3] Current Address: Faculty of Forestry, Lakehead University, 955 Oliver Road, Thunder Bay, Ontario P7B 5E1, Canada

[4] Author to whom correspondence should be addressed

Summary A coupled photosynthesis–stomatal conductance model was parameterized and tested with branches of black spruce (*Picea mariana* (Mill.) B.S.P.) and jack pine (*Pinus banksiana* Lamb.) trees growing in the Northern Study Area of the Boreal Ecosystem–Atmosphere Study (BOREAS) in Manitoba, Canada. Branch samples containing foliage of all age-classes were harvested from a lowland old black spruce (OBS) and an old jack pine (OJP) stand and the responses of photosynthesis (A_n) and stomatal conductance (g_s) to temperature, CO_2, light, and leaf-to-air vapor pressure difference (VPD) were determined under controlled laboratory conditions at the beginning, middle, and end of the growing season (Intensive Field Campaigns (IFC) 1, 2, and 3, respectively). The parameterized model was then tested against *in situ* field gas-exchange measurements in a young jack pine (YJP) and an upland black spruce (UBS) stand as well as in the OBS and OJP stands.

Parameterization showed that Rubisco capacity (V_{max}), apparent quantum yield (α') and Q_{10} for sink limitation were the most crucial parameters for the photosynthesis sub-model and that V_{max} varied among different measurement series in the laboratory. Verification of the model against the data used to parameterize it yielded correlation coefficients (r) of 0.97 and 0.93 for black spruce and jack pine, respectively, when IFC-specific parameters were used, and 0.77 and 0.87 when IFC-2 parameters were applied to all IFCs. For both measured and modeled g_s, the stomatal conductance sub-model, which linearly relates g_s to $(A_n h_s)/c_s$ (where h_s and c_s are relative humidity and CO_2 mole fraction at the leaf surface, respectively), had significantly steeper slopes and higher r values when only the VPD response data were used for parameterization than when all of the response data were used for parameterization.

Testing the photosynthesis sub-model against upper canopy field data yielded poor results when laboratory estimates of V_{max} were used. Use of the mean V_{max} estimated for all upper canopy branches measured on a given day improved model performance for jack pine (from a nonsignificant correlation between measured and modeled A_n to $r = 0.45$), but not for black spruce ($r = 0.45$ for both cases). However, when V_{max} was estimated for each branch sample individually, the model accurately predicted the 23 to 137% diurnal variation in A_n for all

stands for both the upper and lower canopy. This was true both when all of the other parameters were IFC-specific ($r = 0.93$ and 0.92 for black spruce and jack pine, respectively) and when only mid-growing season (IFC-2) values were used ($r = 0.92$ for both species). Branch-specific V_{max} estimates also permitted accurate prediction of field g_s ($r = 0.75$ and 0.89 for black spruce and jack pine, respectively), although parameterization with all of the response data overestimated g_s in the field, whereas parameterization with only the VPD response data provided unbiased predictions. Thus, after parameterization with the laboratory data, accurately modeling the range of A_n and g_s encountered in the field for both black spruce and jack pine was reduced to a single unknown parameter, V_{max}.

Keywords: black spruce, environmental controls on gas exchange, jack pine.

Introduction

Photosynthesis and transpiration are important physiological processes of plants that influence the fluxes of energy, mass and momentum between a vegetated land surface and the atmosphere. These processes can have a profound impact on climatic conditions at the Earth's surface (Sellers et al. 1986, Sato et al. 1989, Margolis and Ryan 1997, Sellers et al. 1997). An improved ability to model the effects of environmental conditions on photosynthesis and transpiration can enhance the precision of both numeric weather prediction models and the simulation of longer-term climate change (Sellers et al. 1986, 1996a, 1996b, 1997). Sellers and coworkers have developed a land surface process model called SiB (Simple Biosphere Model) that accounts for these physiological processes within an atmospheric general circulation model (GCM) (Sellers et al. 1986). They revised SiB (SiB2) to include a coupled photosynthesis–stomatal conductance model (Collatz et al. 1991) that realistically describes the interactions between photosynthesis and transpiration of the vegetation with the physical climate system (Sellers et al. 1992, 1996b).

The boreal forest is one of the two largest terrestrial ecosystems on the planet (Bonan and Shugart 1989). Several model-

ing studies have suggested that increases in radiatively active trace gases such as CO_2 could have a significant impact on climatic conditions in the boreal forest region (e.g., Mitchell 1983, Tans et al. 1990, Sellers et al. 1992, 1996a). These climatic changes could in turn influence physiological processes of the forest (Davies and Botkin 1985, Solomon and Webb 1985, Dang et al. 1997a). Realistic and accurate modeling of photosynthesis and transpiration by the boreal forest at large spatial scales will help us to estimate better the potential impacts of climate change on net primary productivity as well as on carbon and water exchanges between the boreal forest and the atmosphere (Field et al. 1995, Sheriff et al. 1996).

An interesting feature of the coupled photosynthesis–stomatal conductance model in SiB2 is its ability to function at spatial scales ranging from individual leaves to 5,000–10,000 km^2 GCM grid cells. Rigorous testing of the photosynthesis–stomatal conductance model, however, is most readily done either at the individual branch level where standard gas exchange measurements can be easily made or at the stand level using estimates of stand level photosynthesis and transpiration derived from eddy covariance measurements (e.g., Aber et al. 1996). In this study, we parameterized and tested the coupled photosynthesis–stomatal conductance model that is used in SiB2 (Collatz et al. 1991, Sellers et al. 1996b) for branches of black spruce (*Picea mariana* (Mill.) B.S.P.) and jack pine (*Pinus banksiana* Lamb.). Data used for the parameterization were obtained under controlled environmental conditions in the laboratory on samples harvested from a mature lowland black spruce and a mature jack pine stand in the Northern Study Area (NSA) of the Boreal Ecosystem–Atmosphere Study (BOREAS) (Sellers et al. 1995). We then tested the parameterized model against *in situ* field gas-exchange measurements from the same two stands and two additional stands—an upland black spruce and a young jack pine stand.

Materials and methods

Study area

The study was conducted in the NSA of the Boreal Ecosystem–Atmosphere Study (BOREAS) (see Sellers et al. 1995 for details), which is located between Nelson House and Thompson, Manitoba, Canada (56° N, 99° W). The forests in this region consist primarily of black spruce (*Picea mariana*) with some jack pine (*Pinus banksiana*) and smaller patches of trembling aspen (*Populus tremuloides* Michx.). The landscape is a mosaic of low-relief terrain, moderate-sized hills, and small lakes. The soils are derived predominantly from glacial sediments of Lake Agassiz and consist of clays, organic materials and some sandy deposits. Treed peatlands dominated by black spruce are common in lowland areas, whereas jack pine stands are common on sandy glacial outwashes.

Data for parameterization of the photosynthesis–stomatal conductance model

Responses of foliar gas exchange to photosynthetically active radiation (PAR), leaf temperature, intercellular CO_2 concentration, and leaf-to-air water vapor pressure difference (VPD)

were measured under controlled laboratory conditions on cut branches. Branch samples were harvested from the upper canopy of the old black spruce (OBS) and the old jack pine (OJP) stands (see Dang et al. 1997a, 1997b for a detailed description of these stands). Dang et al. (1997a) have shown that gas exchange of detached samples is relatively stable for up to 14 h after harvesting if certain precautions are taken to maintain the physiological integrity of the sample. Therefore, all of the physiological responses in this study were measured within this 14-h time frame. Measurements were taken during the three Intensive Field Campaigns (IFC) of BOREAS in 1994: IFC-1 ran from May 24 to June 16, IFC-2 from July 19 to August 8, and IFC-3 from August 30 to September 19.

For each response curve, samples were harvested with a 12-gauge shotgun from five trees between 0500 and 0700 h. Immediately after harvesting, the stem of each sample was recut under water and the cut surface was kept submerged until the time of measurement. The foliage was kept above the water surface by means of a polystyrene board support structure inside a cooler filled with water.

Gas exchange was measured with an open gas exchange system consisting of a Li-Cor 6262 infrared gas analyzer (Li-Cor, Inc., Lincoln, NE) equipped with two 4-l leaf cuvettes and an environmental control system (Yue et al. 1992). The samples contained foliage of all age-classes. Humidity or water vapor pressure inside the cuvette was controlled by passing saturated air (100% relative humidity) through a series of temperature-controlled condensers. To obtain very low humidities for the measurement of VPD responses, a portion or all of the air was passed through a column of desiccant.

The air temperature inside the leaf cuvette was controlled by circulating a coolant of known temperature from a water bath through radiators. Precautions were taken to avoid water vapor condensing on the radiators at low temperatures. The VPD response was measured at 15, 25, and 35 °C in IFC-1, at 25 and 35 °C in IFC-2, and at 25 °C only in IFC-3. The PAR and CO_2 responses were measured at 20 °C.

The air source for the measurements was ambient air taken from 15 m above the ground with an air sampling tower and an air compressor. A 0.5-m^3 mixing box as well as the reservoir on the compressor were used as buffers to prevent abrupt changes in CO_2 concentration of the input air to the cuvette. Higher than ambient CO_2 concentrations were achieved by mixing ambient air with 10% compressed CO_2 in air. Lower than ambient CO_2 concentrations were obtained by passing a portion of the air through soda lime. The CO_2 concentration was measured with a Li-Cor 6262 in differential mode with standard gases (CO_2 in air) as the reference. The standard gases had in turn been calibrated against the BOREAS primary standard gas by gas chromatography. The difference in water vapor concentration between the air entering and leaving the cuvette was measured with the Li-Cor 6262 in differential mode.

Photosynthetically active radiation was supplied by two 1000-watt high-pressure sodium lamps. To reduce heating in the cuvette, the light was passed through an 8-cm thick filter filled with water before reaching the foliage. The PAR flux

density was varied by using neutral density filters and adjusting the distance between the light source and the leaf chamber. A PAR of 1100 µmol m^{-2} s^{-1} was used to measure the responses of photosynthesis to CO_2, temperature, and VPD. Environmental conditions inside the leaf cuvettes were monitored continuously with a computerized MT-1000 system (Measurement Technology, Inc., Stoughton, MA).

All samples were kept in darkness with the cut surface of the stem submerged in water. The measurement samples, however, were exposed to 700 µmol m^{-2} s^{-1} PAR for 2 h before measurement to induce photosynthetic activity and stomatal opening. Independent pairs of branch samples were used for each value of the environmental factors (i.e., CO_2, temperature and VPD), except in the case of PAR where each sample was exposed to PAR values from 0 to 1450 µmol m^{-2} s^{-1} in descending steps. To keep an adequate water supply to the foliage during the measurement, the cut end of the stem was connected to a water reservoir.

In summary, data for parameterizing the photosynthesis–stomatal conductance model were collected over a wide range of environmental conditions, i.e., temperature ranged from −5 to 35 °C, PAR ranged from 0 to 1450 µmol m^{-2} s^{-1}, CO_2 mole fraction at the leaf surface ranged from 50 to 900 µmol mol^{-1}, and VPD ranged from 0.5 to 5.2 kPa. Only one response curve for one species was measured per day. The VPD response was obtained only at a single temperature on a given day.

The hemi-surface area of the foliage for 25% of the total samples of each species was determined by volume displacement (Brand 1987). The shape factors used to calculate leaf area were 4.00 for black spruce and 4.59 for jack pine. Foliage was then oven-dried and specific leaf area (cm^2 fresh leaf g^{-1} dry leaf) was determined. The hemi-surface area for each of the remaining samples was calculated by multiplying the mean specific leaf area of the first 25% of the samples (separately for each IFC and each species) by foliage dry mass. Net photosynthetic rate (A_n), stomatal conductance (g_s) and intercellular CO_2 concentration (c_i) were calculated according to von Caemmerer and Farquhar (1981). Only steady-state gas exchange values were used for the calculations.

Data for testing the photosynthesis–stomatal conductance model

To test the model, diurnal variations in *in situ* gas-exchange parameters and associated ambient environmental conditions were measured in a young jack pine (YJP) and an upland black spruce (UBS) stand (see Dang et al. 1997*b* for detailed descriptions) as well as in the OJP and OBS stands from which branch samples were taken for model parameterization. Measurements were taken on clear or partially cloudy days with a portable gas exchange system (LI-6200, Li-Cor, Inc.) equipped with a 0.25-l cuvette. Measurements in the OJP, OBS and UBS stands were made from canopy access towers, whereas foliage in the YJP stand was measured from a ladder. Two canopy levels (i.e., upper and lower) of each of the four stands were measured during all three BOREAS IFCs in 1994. One branch section per canopy level was measured for each of the five trees selected at each stand. The same branch sections were meas-

ured repeatedly at about 1-h intervals throughout the day. At the end of the day, the measured branch sections were harvested for determination of leaf area as described earlier. Measurements were taken on June 5, August 5 and September 7 for the OBS stand, August 3 and September 14 for the UBS stand, June 1, July 27, August 9 and 31 for the OJP stand, and May 27, August 1, September 1 and 10 for the YJP stand.

Photosynthesis, stomatal conductance and intercellular CO_2 concentration were calculated by the internal program of the LI-6200 gas exchange system.

Description of the photosynthesis sub-model

The coupled photosynthesis–stomatal conductance model used here has been described in detail by Collatz et al. (1991) and Sellers et al. (1996*a*) and is derived from Farquhar et al. (1980). Here we provide a brief description of it. In the model, the actual rate of photosynthesis is calculated from three potential rates; i.e., J_e, the light-limited rate of photosynthesis, J_c, the Rubisco-limited rate, and J_s, the sink-limited rate (Farquhar et al. 1980). We used a modified version of the original equation to calculate J_e:

$$J_e = \alpha' Q_p[(p_i - \Gamma*)/(p_i + 2\Gamma*)], \tag{1}$$

where α' is apparent quantum efficiency of CO_2 uptake for a branch sample (µmol CO_2 mol^{-1} photon incident on the branch) and is equal to the product of intrinsic quantum efficiency for CO_2 uptake in the absence of photorespiration and leaf absorptance to PAR. The combination of these two parameters into an apparent quantum efficiency was necessary because the architecture of the conifer branches makes estimates of leaf absorptance of PAR difficult to obtain. Additionally, Q_p is PAR flux density (µmol m^{-2} s^{-1}); p_i is the CO_2 partial pressure in the intercellular spaces of the leaves (Pa) and is calculated as:

$$p_i = Pc_i, \tag{2}$$

where P is mean atmospheric pressure measured in the laboratory (97.5 kPa) and c_i is intercellular CO_2 concentration (mol mol^{-1}) as calculated from gas exchange measurements. The parameter $\Gamma*$ is the CO_2 compensation point (Pa) due to photorespiration and is calculated as:

$$\Gamma* = 0.5[O_2]/\tau, \tag{3}$$

where $[O_2]$ is O_2 partial pressure in the intercellular space (20.9 kPa) and τ is the relative specificity of Rubisco to CO_2 relative to O_2 (2600 at 25 °C, $Q_{10,\tau} = 0.57$).

The Rubisco-limited rate of photosynthesis, J_c, is calculated as:

$$J_c = [V_{max}(p_i - \Gamma*)]/[p_i + K_c(1 + [O_2]/K_o)], \tag{4}$$

where V_{max} is the capacity of Rubisco for CO_2 fixation per unit leaf area (µmol m^{-2} s^{-1}); K_c and K_o are, respectively, the Michaelis constant for CO_2 and the competitive inhibition

constant for O_2 with respect to CO_2 in the Rubisco reaction. The constant K_c is taken to be 30 Pa at 25 °C with a Q_{10,K_c} of 2.1 and K_o is taken to be 30 kPa at 25 °C with a Q_{10,K_o} of 1.2 (Collatz et al. 1991). The constants K_c, K_o and τ are adjusted for leaf temperatures other than 25 °C by multiplying the parameter by $Q_{10}^{((T_L - 25)/10)}$ where T_L is leaf temperature (°C).

As described by Sellers et al. (1996b), the adjustment of V_{max} to temperatures other than the 20 °C temperature at which we took our laboratory light and CO_2 response measurements ($V'_{max(adj)}$) is calculated as:

$$V'_{max(adj)} = \frac{V_{max} Q_{10,Rub}((T_L - 20)/10)}{1 + \exp(s_1(T_L - s_2))}, \qquad (5)$$

where V_{max} is the capacity of Rubisco for CO_2 fixation at 20 °C; $Q_{10,Rub}$ is the Q_{10} for Rubisco of 2.4; and s_1 and s_2 are empirical parameters that describe the high temperature inhibition of Rubisco, i.e., s_1 describes the rate of decrease in $V'_{max(adj)}$ with increasing temperature (°C^{-1}) and s_2 (°C) defines the temperature at which $V'_{max(adj)}$ is one-half that at nonstressful temperatures. The high-temperature inhibition term, $1/[1 + \exp(s_1(T_L - s_2))]$, varies between 0 and 1 and describes the decrease in $V'_{max(adj)}$ as a result of enzyme degradation at high temperatures. It has no effect at temperatures within or below the unstressed range.

The sink-limited rate of photosynthesis, J_s, is defined as:

$$J_s = V_{max}/y, \qquad (6)$$

where y is an empirical parameter and represents the maximum rate of unstressed photosynthesis under saturating conditions for PAR and CO_2.

A low-temperature inhibition term, $1/[1 + \exp(s_3(s_4 - T_L))]$, is introduced to J_s in the following equation:

$$J_s = \frac{[V_{max}/y][Q_{10,J_s}((T - 25)/10)]}{[1 + \exp(s_3(s_4 - T_L))]}, \qquad (7)$$

where Q_{10,J_s} is the Q_{10} for the sink limitation, and s_3 and s_4 are equivalent to s_1 and s_2, respectively, but for the low temperature inhibition of J_s.

After the three potential rates (J_e, J_c and J_s) are determined, the actual rate of photosynthesis is calculated by solving two quadratic equations for their smaller roots. This allows a more realistic, gradual transition from one limitation to another when co-limitation by more than one factor occurs (Collatz et al. 1991). The first quadratic (Equation 1) is solved for an intermediate variable, J_p, which is an estimate of photosynthetic rate under the co-limitation of electron transport and Rubisco capacity:

$$\theta J_p^2 - J_p(J_e + J_c) + J_e J_c = 0, \qquad (8)$$

where θ is an empirical constant describing the transition between the two limitations. Next, J_p and J_s are introduced into a second quadratic equation (Equation 9), the smaller root of which is an estimate of the actual rate of gross photosynthesis (A):

$$\beta A^2 - A(J_p + J_s) + J_p J_s = 0, \qquad (9)$$

where β is an empirical constant describing the transition between J_p and J_s. The rate of net photosynthesis (A_n) is then calculated by subtracting dark respiration (R_d) from gross photosynthesis (A). Dark respiration rate at 20 °C was estimated from the light response data at zero light and adjusted for actual measurement temperatures using Q_{10,R_d} values measured by Ryan et al. (1997) on the same species and at the same sites, i.e., 2.1 for black spruce and 2.0 for jack pine.

In summary, the photosynthesis sub-model is driven by three variables—PAR flux density (Q_p), intercellular CO_2 partial pressure (p_i) and leaf temperature (T_L). There are two sets of parameters. The values of the first set of parameters are not adjusted, i.e., Γ^*, τ, K_c, K_o, $Q_{10,\tau}$, Q_{10,K_c}, Q_{10,K_o}, and $Q_{10,Rub}$, and are defined by the biochemistry of photosynthesis at an intercellular O_2 partial pressure of 20.9 kPa (Collatz et al. 1991). The values of the second set of parameters, i.e., α', V_{max}, $V'_{max(adj)}$, θ, β, y, Q_{10,J_s}, s_1, s_2, s_3 and s_4, are estimated from the gas exchange data as described in the following section.

Parameterization of the photosynthesis sub-model

Parameter estimation was conducted using the Marquardt-Levenberg nonlinear regression algorithm in the curve-fitting program of SigmaPlot 2.0 for Windows (Jandel Scientific Inc., San Raphael, CA). To run the program, all parameters had to be assigned an initial estimate. The program then estimates values for one or more parameters that best fit the data by minimizing the sum of the squares differences between the values of the observed and predicted dependent variables through iteration. Because estimating more than one parameter at a time often gave unrealistic results and sometimes resulted in high dependencies between parameters, we estimated one parameter at a time. The response curve (i.e., light, CO_2 or temperature) that gave the most precise estimate of a given parameter was used to fit that parameter. For example, at a nonstressful temperature of 20 °C, light response curves were first used to fit α', θ, α, and $V_{max,light}$. Then, CO_2 response curves were used to fit β, y, and V_{max,CO_2}. The light response parameters, i.e., α', θ, and $V_{max,light}$, were then re-estimated using the newly estimated β and y parameters and then the CO_2 response parameters (i.e., β, y, and V_{max,CO_2}) were in turn re-estimated based on the newly estimated α', θ, and $V_{max,light}$. This process was repeated until stable values were obtained for all of the parameters. Once all of these parameters were set, temperature response curves were used to estimate $V_{max,temp}$, Q_{10,J_s}, s_1, s_2, s_3 and s_4 (one at a time through several cycles until all parameter values were stable). All the parameters were estimated separately for each IFC. The asymptotic standard errors produced by the SigmaPlot curve fitting program were used to calculate a 95% asymptotic confidence interval for each estimated parameter. Dark respiration, R_d, was calculated by averaging A_n when PAR was zero.

To obtain estimates of V_{max} for branches in the field, the SigmaPlot parameterization program was run using A_n, c_i, PAR, T_L from field measurements and the parameters estimated from laboratory measurements.

Description of the stomatal conductance sub-model

Stomatal conductance (g_s) was modeled as:

$$g_s = m[(A_n h_s)/c_s] + b, \qquad (10)$$

where m and b are empirical constants estimated by linear regression, A_n is the net rate of photosynthesis, and h_s and c_s are the relative humidity and CO_2 mole fraction at the leaf surface, respectively. As suggested by Ball et al. (1987), data with CO_2 below 100 µmol mol^{-1} or PAR below 50 µmol m^{-2} s^{-1} were not used to estimate m and b in Equation 10.

Two parameterizations of the stomatal conductance sub-model were conducted. The first parameterization used data pooled from all response curves measured in the laboratory; the second parameterization used only the VPD response data (i.e., VPD from all measurement temperatures and all three IFCs).

Verification and testing of the photosynthesis--stomatal conductance model

The general behavior of the model was first verified by determining how well it predicted the laboratory data that were used to parameterize it. We then tested both the photosynthesis sub-model and the stomatal conductance sub-model against the *in situ* field gas-exchange measurements obtained from the four stands.

To test the photosynthesis sub-model, parameters that were derived totally from the laboratory data for each IFC were used to calculate directly the modeled rate of photosynthesis in the field with PAR, leaf temperature, and intercellular CO_2 concentration measured in the field as input variables (no iteration was necessary because c_i was a measured input variable). We then tested the photosynthesis sub-model by fitting a V_{max} for each field data set (i.e., all measurements in the same stand taken on the same day), but used laboratory-estimated values for all of the other parameters. Finally, we tested the photosynthesis sub-model by fitting a V_{max} for each field sample but as before, all other parameters were estimated from the laboratory data.

To test the stomatal conductance sub-model, we used two parameterizations of the model (both from laboratory data) to calculate modeled stomatal conductance in the field directly. The first parameterization used all of the laboratory response data (i.e., light, CO_2, temperature and VPD responses), whereas the second used only the VPD response data. This was done to test how the stomatal conductance model would perform when parameterized with only VPD, which is the most important factor influencing stomatal conductance in the field (Dang et al. 1997a), compared with its performance when parameterized with a wide range of environmental response data. Model-predicted A_n and field-measured h_s and c_s were used in these tests.

Statistical analysis

The asymptotic 95% confidence intervals calculated for the photosynthetic parameters (V_{max}, α', θ, β, y, Q_{10, J_s}, s_1, s_2, s_3 and s_4) were used to evaluate whether parameter values were significantly different between IFCs. Statistically significant differences in the linear slope parameter, m, of the conductance model were determined by a z-test at a threshold of $P = 0.05$, i.e., slopes were considered not significantly different from each other when $P > 0.05$. Similarly, analyses of whether the slope of the modeled versus measured A_n or modeled versus measured g_s was significantly different from 1.0 were also determined by z-tests at $P = 0.05$. The regression model F-statistic and its associated probability were used to determine whether the intercepts of the linear regressions were significantly different from zero.

Results

Model parameterization with laboratory data

Light response: estimating α', θ, R_d and $V_{max,light}$ The PAR-saturated rate of net photosynthesis was lower in IFC-1 than in IFC-2 and IFC-3 in both black spruce and jack pine, but the difference was greater in black spruce (Figure 1). For both species, photosynthesis appeared to saturate at a lower PAR in IFC-1 than in the other two IFCs (Figure 1). Apparent quantum yield (α') was greatest in IFC-2 for black spruce (Table 1, Figures 1a to 1c), whereas α' did not differ significantly between IFCs for jack pine (Table 1). The co-limitation parameter, θ, derived from the modeled light response curve (solid lines in Figure 1), did not differ between IFCs for black spruce, but was significantly higher in IFC-1 for jack pine (Table 1). However, changes in this parameter made little difference to the shape of the light response curve, indicating that differences in θ between IFCs for jack pine are not biologically significant. Dark respiration at 20 °C averaged 0.63 and 0.69 µmol m^{-2} s^{-1} for black spruce and jack pine, respectively.

For black spruce, $V_{max,light}$ estimated from the light response data in IFC-1 was 47% of the mean $V_{max,light}$ estimated for IFC-2 and IFC-3 (Table 1). For jack pine, the $V_{max,light}$ for IFC-1 was 78% of that estimated for the other two IFCs (Table 1).

Carbon dioxide response: estimating β, V_{max,CO_2} and y
For both species, net photosynthesis (A_n) increased with increasing intercellular CO_2 up to the maximum concentration used in the study (650 µmol mol^{-1}) (Figure 2). The co-limitation factor, which is described by the parameter β, did not differ significantly between IFCs for either black spruce or jack pine (Table 1). The V_{max,CO_2} was similar to $V_{max,light}$ in both magnitude and seasonal trend. For black spruce, V_{max,CO_2} for IFC-1 was 58% of the highest V_{max} (IFC-3), whereas for jack pine V_{max,CO_2} for IFC-1 was 64% that of the highest V_{max,CO_2} (IFC-2) (Table 1).

Sink limitation, described by parameter y, did not differ significantly between IFCs (Table 1).

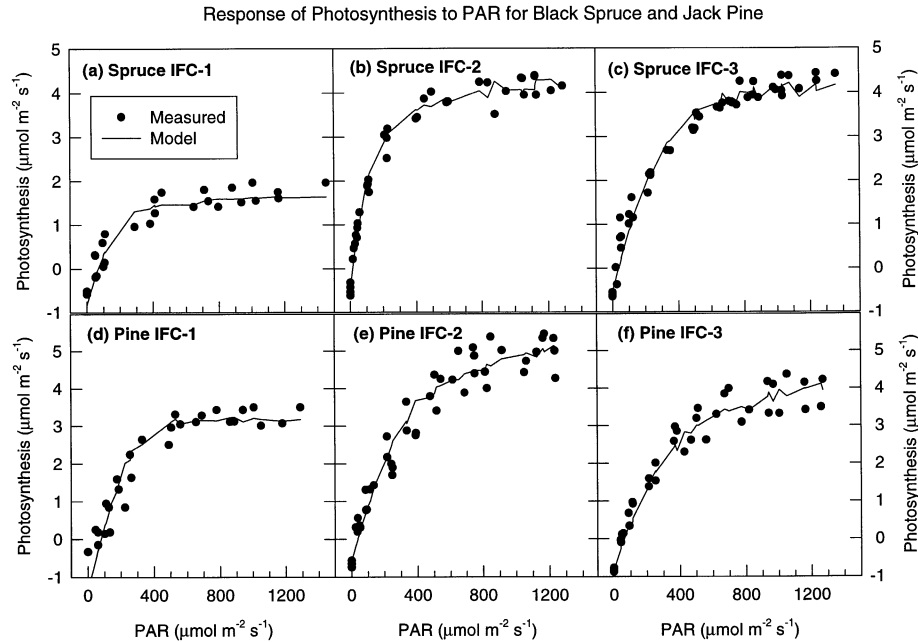Response of Photosynthesis to PAR for Black Spruce and Jack Pine

Figure 1. Response of net photosynthesis to photosynthetically active radiation flux density (PAR) for black spruce and jack pine. Measurements were taken in the laboratory on branch samples harvested from the forest during all three 1994 Intensive Field Campaigns (IFC) of BOREAS.

Table 1. Parameters for the photosynthesis sub-model estimated from laboratory leaf gas-exchange measurements on cut branches for black spruce (OBS) and jack pine (OJP) in the Northern Study Area of BOREAS. Measurements were taken during all three Intensive Field Campaigns (IFC) of BOREAS.

Species	IFC	$V_{max,light}$	V_{max,CO_2}	$V_{max,temp}$	α'	θ	β	y	R_d	Q_{10,J_s}	s_1	s_2	s_3	s_4
OBS	1	7.6 a	9.1 a	9.8 a	0.017 a	0.83 a	0.93 a	1.58 a	0.80	1.99 a	2.59 a	38.0 a	0.17 a	−0.7 a
	2	15.0 b	12.1 a,b	18.0 b	0.040 b	0.70 a	0.93 a	1.36 a	0.48	1.22 b	1.56 a,b	44.0 b	0.32 a	4.3 b
	3	17.4 b	15.7 b	11.8 a	0.020 a	0.86 a	0.81 a	1.77 a	0.60	0.74 c	0.66 b	36.4 a	0.54 a	0.2 a
	Mean	13.4	12.3	13.2	0.026	0.80	0.89	1.57	0.63	1.32	1.60	39.5	0.34	1.3
OJP	1	15.1 a	12.9 a	13.6 a	0.022 a	0.95 a	0.73 a	1.98 a	0.55	0.95 a	0.19 a	35.3 a	1.08 a	−3.02 a
	2	20.7 b	20.2 b	14.2 a	0.021 a	0.75 b	0.92 a	1.46 a	0.68	0.99 a	0.26 a	36.3 a	0.32 b	2.40 b
	3	18.0 a,b	14.7 a	14.4 a	0.018 a	0.78 b	0.90 a	2.30 a	0.83	1.40 b	1.05 b	37.0 a	0.30 b	3.20 b
	Mean	18.7	17.0	15.3	0.020	0.83	0.85	1.85	0.69	1.19	0.46	35.1	0.53	0.94

Abbreviations: V_{max} = Rubisco capacity (μmol m^{-2} s^{-1}); $V_{max,light}$ = V_{max} from light response data; V_{max,CO_2} = V_{max} from CO_2 response data; $V_{max,temp}$ = V_{max} from temperature response data; α' = apparent quantum efficiency (Equation 1; mol CO_2 mol^{-1} photon absorbed); θ and β = model parameters as described in Equations 8 and 9; y = coefficient for sink limitation (Equation 6); R_d = dark respiration rate at 20 °C (μmol m^{-2} s^{-1}); Q_{10,J_s} = Q_{10} for sink limitation; s_1 to s_4 = parameters for temperature limitations where s_1 and s_3 are in °C^{-1} and s_2 and s_4 are in °C (see Equations 5 and 7). The Q_{10} for R_d is 2.1 for black spruce and 2.0 for jack pine (Ryan et al. 1997). Parameters whose units are not defined above are unitless. For the same parameter and species, values with different letters are significantly different using the 95% asymptotic confidence interval (see Materials and methods).

Temperature response: estimating s_1, s_2, s_3, s_4, β and Q_{10,J_s}

Net photosynthetic rate was only slightly limited by temperature between approximately 10 and 33 °C for both species and for all IFCs (Figure 3). During IFC-1, jack pine appeared to be capable of maintaining almost optimum photosynthetic rates at temperatures slightly above 0 °C (Figure 3).

As for the V_{max} estimates derived from the light and CO_2 response data, $V_{max,temp}$ was lowest in IFC-1 for black spruce (Table 1); however, unlike the other estimates of V_{max}, $V_{max,temp}$ was also significantly lower in IFC-3 than in IFC-2 for

black spruce. There were no significant differences in $V_{max,temp}$ between IFCs for jack pine.

The two parameters (s_3 and s_4) that are supposed to define the decrease in V_{max} and thus A_n at low temperatures had only a minor influence on the shape of the temperature response curve. Rather, the dominant parameter in the model influencing the shape of the temperature response curve was Q_{10,J_s}, i.e., the Q_{10} for the temperature response of sink limitation (J_s). This parameter decreased from IFC-1 to IFC-3 in black spruce but increased from IFC-1 to IFC-3 in jack pine (Table 1).
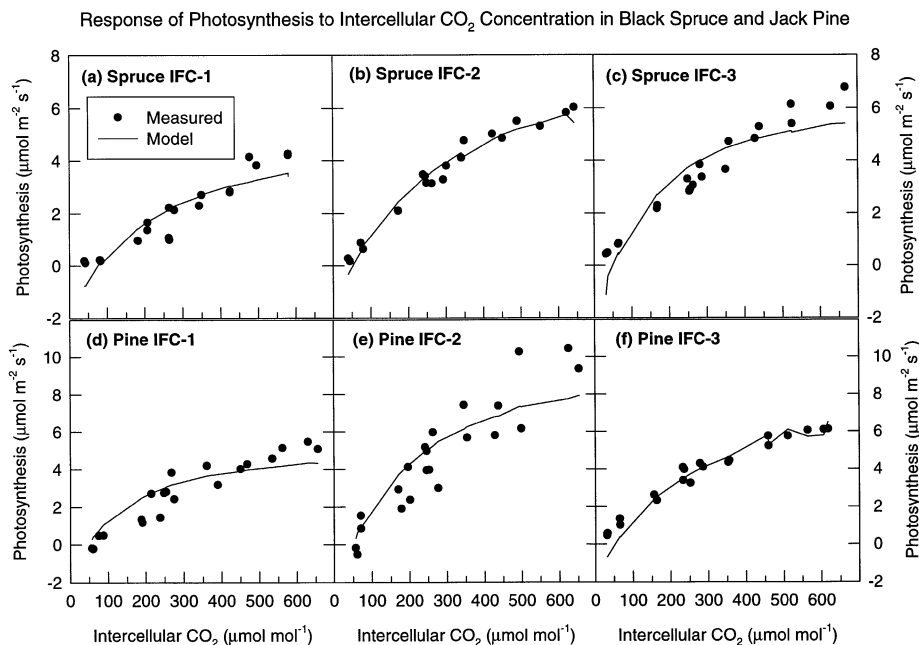
Response of Photosynthesis to Intercellular CO$_2$ Concentration in Black Spruce and Jack Pine

Figure 2. Response of net photosynthesis to intercellular CO$_2$ concentration for black spruce and jack pine measured in the laboratory. Measurements were taken in the laboratory on branch samples harvested from the forest during all three 1994 Intensive Field Campaigns (IFC) of BOREAS.

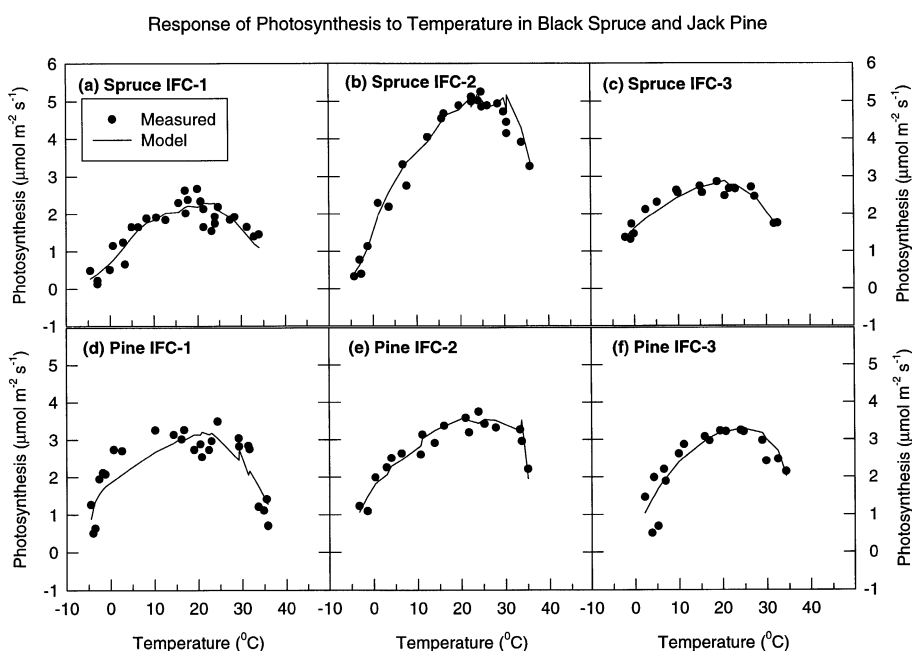Response of Photosynthesis to Temperature in Black Spruce and Jack Pine

Figure 3. Response of net photosynthesis to temperature for black spruce and jack pine measured in the laboratory. Measurements were taken in the laboratory on branch samples harvested from the forest during all three 1994 Intensive Field Campaigns (IFC) of BOREAS.

The two parameters that are supposed to define the decrease in V_{max} and thus A_n at high temperatures (s_1 and s_2) also had a relatively small effect on the shape of the temperature response curve. In the model, the decrease in A_n at temperatures above 30 °C was driven primarily by an exponential increase in respiration and to some extent by an increase in Γ^* (Equation 4). Parameter s_2, which defines the temperature at which $V'_{max(adj)}$ attains half of its value at 20 °C, was beyond the range of the temperature data used for the measurements, i.e., > 35 °C (Table 1).

Verifying the photosynthesis sub-model with laboratory data

The photosynthesis sub-model captured most of the variation in the laboratory-measured A_n for the PAR response, the CO$_2$ response, and the temperature response (Figure 4). Modeled A_n was significantly ($P < 0.05$) and linearly correlated to measured A_n for both species (Figure 4). When parameters specific to each IFC were used, the correlation coefficient was 0.97 for black spruce and 0.93 for jack pine (Figures 4a and 4b). The slope of this relationship was not significantly different from one ($P > 0.05$) for either species. When the parameters

derived from the IFC-2 data were applied to the data from all three IFCs, the correlation coefficient decreased to 0.77 for black spruce and to 0.87 for jack pine (Figures 4c and 4d). Furthermore, the slope was significantly less than one for both species ($P < 0.05$) (Figures 4c and 4d), indicating that the IFC-2 parameterization overestimated photosynthesis for both IFC-1 and IFC-3, but particularly for IFC-1.

Verifying the stomatal conductance sub-model with laboratory data   Laboratory-measured g_s was significantly ($P < 0.05$) and linearly correlated with measured $A_n h_s/c_s$ both when all response data were used and when only the VPD response data were used (Figure 5). When all of the data were combined, the correlation coefficient was 0.82 for black spruce and 0.81 for jack pine (Figures 5a and 5b). When only VPD response data were used, the correlation coefficient increased to 0.91 for black spruce and to 0.90 for jack pine (Figures 5c and 5d). The slope of the relationship was significantly greater for the VPD response data than it was for all of the data combined ($P < 0.05$, Figures 5a and 5b versus 5c and 5d, respectively).

For both species, modeled g_s (using modeled A_n and the m and b conductance parameters) was significantly ($P < 0.05$) and linearly correlated with laboratory-measured g_s both when the model was parameterized with all of the data (Figures 6a and 6b) and when it was parameterized only with the VPD response data (Figures 6c and 6d). However, the correlation coefficient was greater when only the VPD response data were

Figure 5. Relationship between stomatal conductance (g_s) and the combined effects of net photosynthesis (A_n), relative humidity at the leaf surface (h_s) and CO_2 concentration at the leaf surface (c_s) for (a and c) black spruce and (b and d) jack pine. Responses to PAR, CO_2, temperature and VPD were all combined in (a) and (b), whereas only the VPD response data were used in (c) and (d). Data were collected during all three 1994 Intensive Field Campaigns (IFC) of BOREAS.
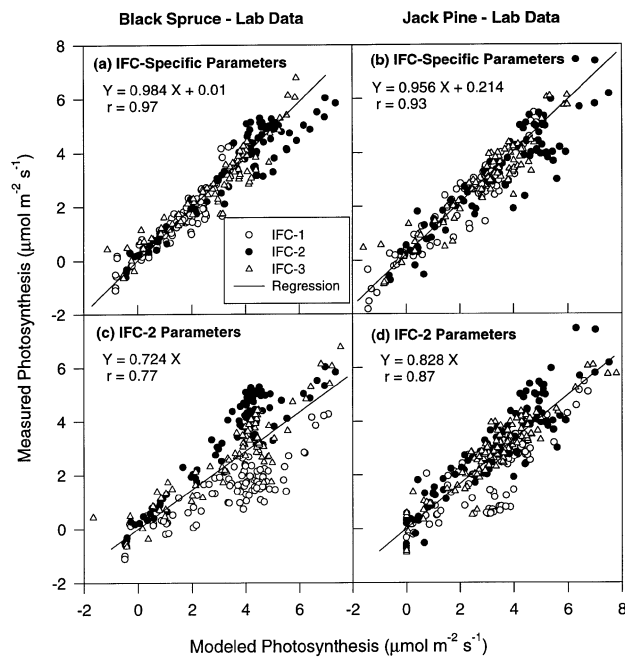

Figure 4. Relationship between modeled net photosynthesis and the net photosynthesis measured in the laboratory on branch samples of (a and c) black spruce and (b and d) jack pine harvested from the forest. Data were collected during all three 1994 Intensive Field Campaigns (IFC) of BOREAS. IFC-specific model parameters were used in (a) and (b), whereas IFC-2 model parameters were applied to all three IFCs in (c) and (d).
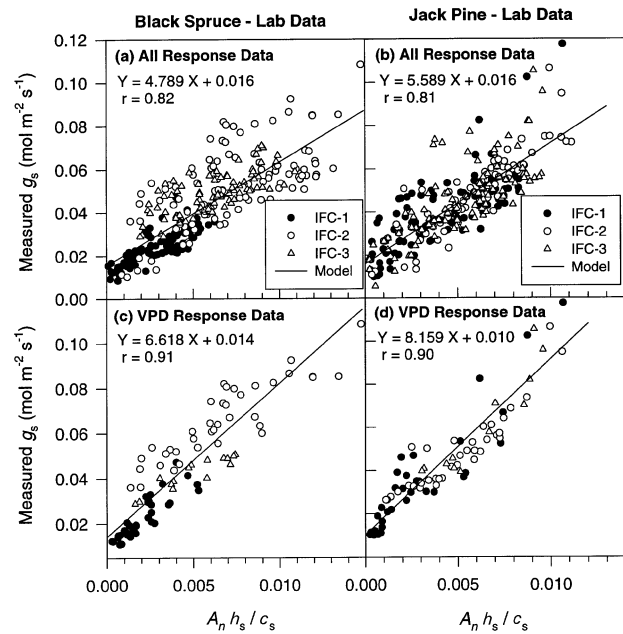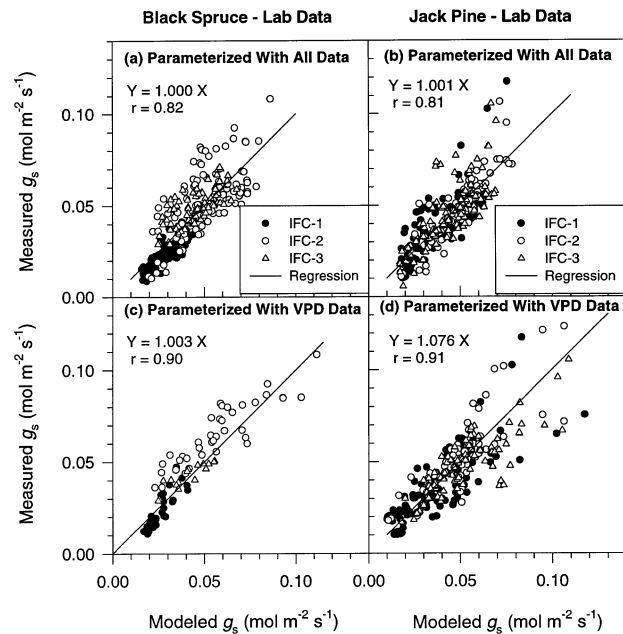

Figure 6. Relationship between modeled stomatal conductance (g_s) (using modeled A_n and the m and b conductance parameters) and g_s measured in the laboratory on branch samples of jack pine and black spruce harvested from all three 1994 Intensive Field Campaigns (IFC) of BOREAS. The responses to PAR, CO_2, temperature and VPD were all combined in (a) and (b), whereas only the VPD response data were used in (c) and (d).

used than when all of the data were used (Figures 6a and 6b versus Figures 6c and 6d, respectively). The slopes of these relationships were not significantly different from one ($P > 0.05$) and the intercepts were not significantly different from zero ($P > 0.37$) for either parameterization, suggesting that both parameterizations generally provided unbiased predictions of laboratory measured g_s. However, the model underestimated measured g_s at high g_s in jack pine (> 0.09 mol m^{-2} s^{-1}) when parameterized with all of the data (Figure 6b).

Field testing of photosynthesis sub-model

When the model parameterized with IFC-specific parameters derived from the laboratory measurements was compared with the field measurements of the upper canopy, modeled A_n was significantly correlated with field-measured A_n for black spruce ($P < 0.05$, Figure 7a), but not for jack pine ($P > 0.08$, Figure 7b). There was a weak relationship between modeled and measured A_n ($P < 0.05$) for both species when a single V_{max} value was estimated from the field data for each individual data set (measurements of the same stand taken on the same day), whereas all other parameters were as defined from the laboratory data (Figures 7c and 7d).

When V_{max} was estimated for each individual field branch sample (all measurements of the same branch taken on the

same day), modeled A_n was significantly ($P < 0.05$) and linearly correlated to the measured values for both the upper and lower canopy levels (Figures 8a and 8b). The slope of this relationship was not significantly different from one for either species ($P > 0.78$) and the intercept was not significantly different from zero for either species ($P > 0.32$). The relationship was similar when the IFC-2 parameters were applied to all IFCs as when the IFC-specific parameterization was used (Figures 8c and 8d versus Figures 8a and 8b, respectively). The OBS and UBS stands fell along the same line (Figures 8a and 8c), and the OJP and YJP stands also fell along the same line (Figures 8b and 8d).

The value of V_{max} calculated for different field samples measured on the same day varied considerably as did V_{max} of field samples on different days (Table 2). As might be expected, V_{max} was generally lower for lower-canopy foliage than for upper-canopy foliage for black spruce. The V_{max} for lower-canopy foliage of the more open jack pine stands was close to that for upper-canopy foliage, except for the YJP stand on September 10 when lower-canopy foliage showed a V_{max} that was nearly 1.5 times greater than that for upper-canopy foliage. Additionally, V_{max} calculated for the field measurements was generally lower than that for the laboratory data (Tables 1 and 2).
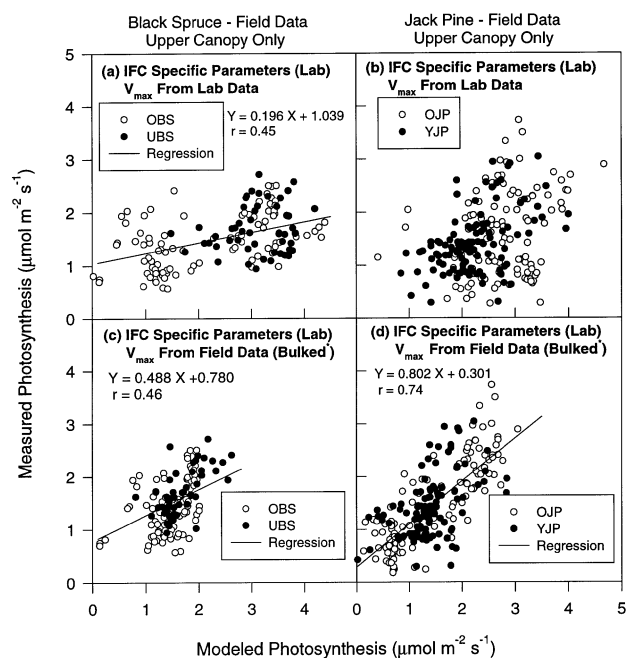

Figure 7. Relationship between modeled net photosynthesis and the net photosynthesis measured in the field on *in situ* branches in the upper canopy of (a and c) black spruce and (b and d) jack pine. Intensive Field Campaign-specific model parameters derived from laboratory measurements were used in (a) and (b). In (c) and (d), V_{max} specific to each day of field measurement was used, whereas other parameters were from the laboratory parameterization. Bulked = a single V_{max} was estimated by the model from all field data collected in the same stand and on the same day. OBS = old black spruce; UBS = upland black spruce; OJP = old jack pine; YJP = young jack pine.
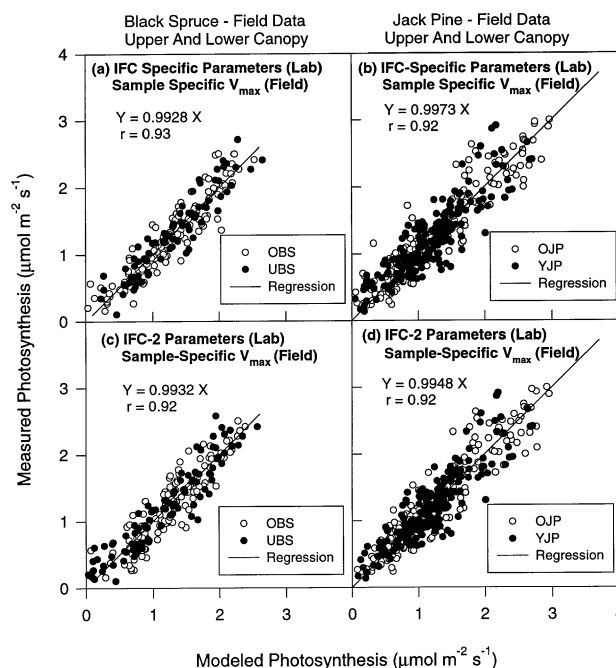
Figure 8. Relationship between modeled net photosynthesis and the net photosynthesis measured in the field on *in situ* samples in both upper and lower canopies of (a and c) black spruce and (b and d) jack pine. The value of V_{max} was estimated for each branch sample from the field measurements and all other model parameters were derived from the laboratory measurements. Intensive Field Campaign-specific model parameters were used in (a) and (b), whereas IFC-2 model parameters were applied to field measurements from all IFCs in (c) and (d). Site abbreviations are as described in Figure 7.

Table 2. Mean, standard error (SE) and range of V_{max} (μmol CO_2 m^{-2} s^{-1}) for old black spruce (OBS), upland black spruce (UBS), old jack pine (OJP) and young jack pine (YJP) field data from the BOREAS Northern Study Area.

Site	Date	Upper canopy		Lower canopy	
		Mean (SE)	Min – max range	Mean (SE)	Min – max range
OBS	June 5	8.5 (0.6)	6.2–12.1	–	–
	August 5	7.2 (0.3)	6.7–7.9	5.5 (0.7)	3.6–6.9
	September 7	9.5 (0.7)	7.6–10.8	8.0 (0.6)	6.7–10.1
UBS	August 3	6.2 (0.4)	5.3–7.1	4.1 (0.3)	3.4–5.0
	September 14	10.6 (0.4)	9.2–11.2	5.5 (0.3)	4.8–6.2
OJP	June 1	4.6 (0.3)	4.0–5.5	–	–
	July 27	7.5 (0.5)	6.5–9.4	6.9 (0.3)	5.3–8.0
	August 9	12.0 (0.4)	10.6–13.2	9.9 (1.5)	6.6–12.7
	August 31	13.0 (1.0)	11.3–15.2	11.3 (0.8)	9.3–13.3
YJP	May 27	8.0 (1.4)	4.3–10.4	8.3 (2.0)	3.8–12.2
	August 1	11.3 (0.7)	8.8–12.6	11.6 (0.8)	9.5–14.0
	September 1	11.0 (0.9)	7.8–12.5	9.1 (0.7)	7.6–11.1
	September 10	9.9 (0.4)	9.2–11.2	14.3 (1.8)	10.2–19.8

Field testing of stomatal conductance sub-model

For both jack pine and black spruce, modeled g_s (using modeled A_n and the m and b conductance parameters) was significantly ($P < 0.05$) and linearly correlated with measured g_s both when parameterized with all of the data or only the VPD response data (Figure 9). The slope of the modeled versus measured g_s relationship, however, was significantly greater than one when the all-data parameterization was used ($P < 0.05$). On the other hand, it was not significantly different from one for the parameterization with only the VPD response data ($P > 0.30$), indicating that the parameterization with only the VPD

Figure 9. Relationship between modeled stomatal conductance (g_s) and g_s measured in the field on *in situ* branches of (a and c) black spruce and (b and d) jack pine. The model was parameterized from all laboratory response data in (a) and (b), whereas it was parameterized from the laboratory VPD response data only in (c) and (d). Site abbreviations are as described in Figure 7.

response data gave unbiased estimates of field g_s, whereas parameterization with all of the data underestimated field g_s. The UBS and OBS stands fell along the same line (Figures 9a and 9c). The OJP and YJP stands also fell along the same line (Figures 9b and 9d).

Discussion

Photosynthesis–stomatal conductance model: parameterization and verification

Parameterization of the photosynthesis sub-model revealed that α', Q_{10,J_s} and V_{max} were crucial parameters for obtaining a good fit of the model to the data that were used to parameterize it (Table 1, Figures 1 to 4). The parameter most critical to the performance of the photosynthesis sub-model was V_{max}, the maximum Rubisco activity per unit leaf area. Because this parameter was so important, it was usually necessary to estimate it for every laboratory measurement series (light, CO_2, temperature) in order to obtain reasonable estimates of the other model parameters. Aber et al. (1996) found that their canopy-level photosynthetic model was also more sensitive to the parameter describing photosynthetic capacity than it was to other model parameters. There were probably several reasons for the large variability we observed in V_{max}. First, there was marked seasonal variation in V_{max}. The estimate of V_{max} early in the growing season (IFC-1) was 17 to 56% and 4 to 36% lower than the mid- and late-growing season values for black spruce and jack pine, respectively (Table 1). This appears to reflect both the gradual activation and dehardening of the previous year's photosynthetic machinery with increasing temperature and the fact that current-year foliage had not yet formed in IFC-1. Second, the variability in V_{max} may be related to horizontal variability within each of the stands. Although foliage was always collected in the same general area of the stands, there was microsite variability. Such variability was most evident in the old black spruce stand where relatively small changes in topography affected both the thickness of the
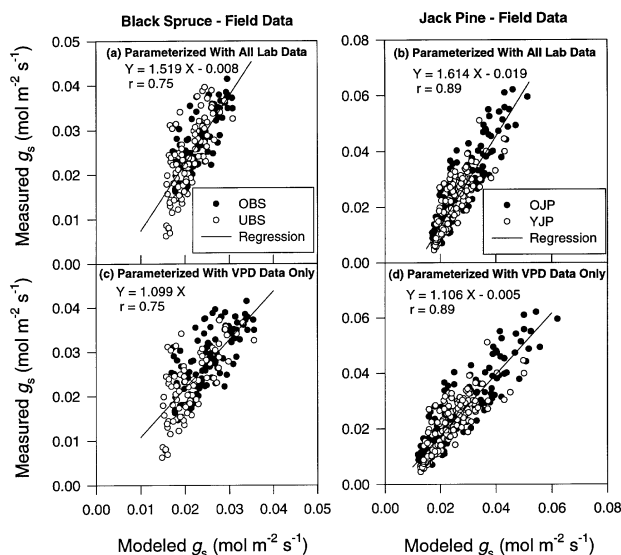
moss layer and tree size. Microsite variability can also affect microbial activity, nitrogen cycling and plant growth (e.g., Van Cleve et al. 1983, Van Cleve and Yarie 1986, Pastor et al. 1987, Tilman 1987), which may in turn affect foliage nitrogen concentration and thus V_{max} values. In the OJP stand, microsite variability appeared to be related primarily to tree density which may in turn be related to soil characteristics. Dang et al. (1997*b*) observed large variations in foliage nitrogen concentration and photosynthetic capacity in both the OJP and OBS stands.

Verification of the photosynthesis sub-model with the laboratory data showed that, despite the variability in certain model parameters over the growing season (Table 1), a single mid-growing season parameterization gave reasonable results (Figure 4c and 4d). However, the correlation coefficients decreased and the slope of modeled A_n versus measured A_n became significantly less than one for both species when the mid-season parameterization was applied to all the measurements ($P < 0.05$; Figure 4).

Verification of the stomatal conductance sub-model, on the other hand, showed that the m parameter describing the slope of the g_s versus $A_n h_s / c_s$ relationship was significantly greater when only the VPD response data were used in the parameterization than when all of the the data were used (Figure 5). Thus, although the model predicts that there should be no difference in the estimate of m from these two data sets, this was clearly not the case. The VPD effect on g_s has been shown to be important in the field (Dang et al. 1997*a*, Hogg and Hurdle 1997, Saugier et al. 1997).

The finding that a model fits the data that were used to parameterize it only indicates that the model functions properly over the range of environmental conditions used. It does not, however, constitute an independent test of model performance.

Field testing

Applying the laboratory-parameterized model to the field measurements initially gave poor results for both black spruce and jack pine (Figures 7a and 7b). A subsequent examination of the field data showed that different branches exposed to the same environmental conditions often had greatly different rates of A_n, e.g., the difference in photosynthetic rates was as high as 200% between different samples that were measured within a short period of time under almost identical environmental conditions (data not presented). This variability was attributed to variations in leaf nitrogen concentration and V_{max}. For this reason, we further examined V_{max} of the field samples.

There was great variation in V_{max} among samples, e.g., the variation was as high as 300% in the lower canopy of YJP in May (Table 2). As well, V_{max} was generally greater for the upper canopy than for the lower canopy, particularly for black spruce (Table 2). Consequently, obtaining good model performance for A_n required obtaining an estimate of V_{max} for each branch measured under field conditions on a given day (Figure 8). Once this was done, the model closely tracked diurnal changes in the field-measured A_n. Diurnal variation in these

A_n measurements ranged from 23 to 137% for black spruce and from 30 to 114% for jack pine depending on the day. Applying the IFC-2 parameterization for all parameters except V_{max} did not change model performance (Figures 8c and 8d).

Additionally, when V_{max} was defined for each branch, the parameterization for photosynthesis of foliage in the upper canopy also worked well for foliage in the lower canopy. Furthermore, parameterization for the OBS and OJP stands accurately described A_n for the UBS and YJP stands as well (Figure 8). Consequently, it appears that, after parameterization with the laboratory data, modeling the range of A_n encountered in the field for both black spruce and jack pine can be reduced to a single unknown parameter, V_{max}.

Interestingly, the adjustments to V_{max} that permitted the photosynthetic model to predict A_n in the field accurately, also enhanced the performance of the stomatal conductance sub-model (Figure 9). Thus, V_{max} is also critical to accurate prediction of g_s.

Our values of V_{max} are within the general range reported for conifers (Wullschleger 1993), but are lower than the values obtained for the same species in the BOREAS Southern Study Area (SSA) 500 km to the south (J. Berry, Carnegie Institution, Stanford, CA, personal communication). The difference in V_{max} between the two study areas might be attributed to differences in climate and soil conditions between the two regions or to specific differences in the sites. The old black spruce site (OBS) in the SSA is better drained and more productive than the NSA site. In 1994, aboveground net primary production (ANPP) was 1347 versus 1618 kg C ha^{-1} year^{-1} for the OBS stands in the north and the south, respectively, whereas the corresponding values for jack pine were 1195 versus 1177 kg C ha^{-1} year^{-1} (Gower et al. 1997).

Except for OBS in IFC-1, V_{max} for the laboratory measurements was greater than that for the corresponding field measurements (Tables 1 and 2). There are at least two possible reasons for this. One reason is that differences in the amount, age-classes, and orientation of the foliage in the field and laboratory cuvettes might have yielded differences in the measured rate of A_n and consequently in the estimate of V_{max}. The laboratory cuvettes were 4 l in size, whereas the cuvettes used for the field measurements were only 0.25 l. The other reason concerns the hydraulic constraint that occurs when large trees move water from the soil up to the foliage (Sperry and Pockman 1993, Saliendra et al. 1995, Sperry 1995). Elimination of this constraint in the cut branches may have resulted in increased V_{max}. Yoder et al. (1994) reported that foliage on tall trees of *Pinus ponderosa* Dougl. ex Laws. and *Pinus contorta* Dougl. ex Loud. had lower conductance and photosynthesis than foliage on shorter trees. Sellers et al. (1996*b*) suggested that water-stress-induced reductions in photosynthesis should be modeled by corresponding reductions in V_{max}. Dang et al. (1997*a*) reported that g_s of laboratory measured cut branches of jack pine was slightly higher than that measured on intact branches in the field at similar VPDs, but there were no significant differences for black spruce.

The large variations in V_{max} among branches, and its critical role in determining the performance of the model places a

constraint on the ease with which the model can be applied to different spatial scales. However, a parameterization might be reliably applied at larger scales if a relatively large sample size is used to estimate average V_{max}. Because V_{max} and leaf photosynthetic capacity are related to leaf nitrogen concentration per unit leaf area, simple measurements of leaf nitrogen along a canopy profile may be sufficient to derive estimates of canopy V_{max} (Field 1991, Dang et al. 1997b). Additionally, light response curves for entire ecosystems that are generated by eddy covariance measurements (e.g., Aber et al. 1996, Baldocchi and Vogel 1996, Black et al. 1996, Baldocchi et al. 1997) can be used to estimate ecosystem V_{max}. It might also be possible to relate V_{max} per unit ground area to remotely sensed spectral vegetation indices such as the normalized difference vegetation index (NDVI), because NDVI is related both to leaf area and to the fraction of PAR absorbed by vegetation. Dang et al. (1997b) related NDVI to photosynthetic capacity per unit ground area in six boreal forest stands, including the four used in this study, and obtained a correlation coefficient of 0.93.

The range of VPDs and the interactions between temperature and VPD were critical to the accurate parameterization of the stomatal conductance sub-model. Both temperature and VPD were kept relatively constant when the light and CO_2 responses were measured (20 ± 0.5 °C, 0.7 ± 0.2 kPa). Vapor pressure difference was also held to a narrow range during measurement of the response of photosynthesis to temperature (0.5 to 1.6 kPa for the temperature range from 10 to 35 °C). The VPD response, on the other hand, was measured over a wide range of VPDs (0.2 to 5.2 kPa) and temperatures (15 to 35 °C). Thus, when all the response data were used to parameterize the stomatal conductance sub-model, data having high and low VPD values were underrepresented. Because VPD and its interaction with temperature are critical factors influencing stomatal conductance (Dang et al. 1997a), the underrepresentation of high and low VPD values could have a substantial impact on the range of environmental conditions to which the model can be applied. The model parameterized from all of the laboratory response data underestimated g_s of the upper canopy in the field, probably because the field data, unlike the all-response laboratory data, were collected over a wide range of VPDs (0.5 to 4.3 kPa). The model parameterized with the VPD response data only, however, provided unbiased predictions of g_s. Collatz et al. (1991) also emphasized the importance of equal weighting of environmental variables over the entire range of environmental conditions when parameterizing a stomatal conductance model.

References

Aber, J.D., P.B. Reich and M.L. Goulden. 1996. Extrapolating leaf CO_2 exchange to the canopy: a generalized model of forest photosynthesis compared with measurements by eddy correlation. Oecologia 106:257–265.

Baldocchi, D.D. and C.A. Vogel. 1996. Energy and CO_2 flux densities above and below a temperate broad-leaved forest and a boreal pine forest. Tree Physiol. 16:5–16.

Baldocchi, D.D., C.A. Vogel and B. Hall. 1997. Seasonal variation of carbon dioxide exchange rates above and below a boreal jack pine forest. Agric. For. Meteorol. 83:147–170.

Ball, J.T., I.E. Woodrow and J.A. Berry. 1987. A model for predicting stomatal conductance and its contribution to the control of photosynthesis under different environmental conditions. *In* Progress in Photosynthesis Research. Vol. 4. Ed. J. Biggins. Nijhoff, Dordrecht, The Netherlands, pp 221–224.

Black, T.A., G. den Hartog, H. Neumann, P. Blanken, P. Yang, Z. Nesic, S. Chen, C. Russell, P. Voroney and R. Stabeler. 1996. Annual cycles of CO_2 and water vapor fluxes above and within a boreal aspen stand. Global Change Biol. 2:219–229.

Bonan, G.B. and H.H. Shugart. 1989. Environmental factors and ecological process in boreal forests. Annu. Rev. Ecol. Syst. 20:1–28.

Brand, D.G. 1987. Estimating the surface area of spruce and pine foliage from displaced volume and length. Can. J. For. Res. 17:1305–1308.

Collatz, G.J., J.T. Ball, C. Givet and J.A. Berry. 1991. Physiological and environmental regulation of stomatal conductance, photosynthesis and transpiration: a model that includes a laminar boundary layer. Agric. For. Meteorol. 54:107–136.

Dang, Q.-L., H.A. Margolis, M.R. Coyea, M. Sy and G.J. Collatz. 1997a. Regulation of branch-level gas exchange of boreal trees: roles of shoot water potential and vapor pressure difference. Tree Physiol. 17:521–535.

Dang, Q.-L., H.A. Margolis, M. Sy, M.R. Coyea, G.J. Collatz and C.L. Walthall. 1997b. Profiles of PAR, nitrogen, and photosynthetic capacity in the boreal forest: implications for scaling from leaf to canopy. J. Geophys. Res. (Atmos.) (D2). 102:28845–28859.

Davies, M.B. and D.B. Botkin. 1985. Sensitivity of cool temperature forests and their fossil pollen to rapid climatic change. Quat. Res. 23:327–340.

Farquhar, G.D., S. von Caemmerer and J.A. Berry. 1980. A biochemical model of photosynthetic CO_2 assimilation in leaves of C_3 plants. Planta 149:78–90.

Field, C.B. 1991. Ecological scaling of carbon gain to stress and resource availability. *In* Response of Plants to Multiple Stresses. Eds. H.A. Mooney, W.E. Winner and E.J. Pell. Academic Press, Inc., San Diego, pp 35–65.

Field, C.B., J.T. Randerson and C.M. Malmstrom. 1995. Global net primary production: Combining ecology and remote sensing. Remote Sens. Environ. 51:74–88.

Gower, S.T., J. Vogel, T.K. Snow, J.M. Norman, S.J. Steele and C.J. Kucharik. 1997. Carbon distribution and above-ground net primary production of upland and lowland boreal forests in Saskatchewan and Manitoba, Canada. J. Geophys. Res. (Atmos.) (D2). 102:29029–29041.

Hogg, E.H. and P.A. Hurdle. 1997. Sap flow in trembling aspen: implications for stomatal responses to vapor pressure deficit. Tree Physiol. 17:501–509.

Margolis, H.A. and M.G. Ryan. 1997. A physiological basis for biosphere–atmosphere interactions in the boreal forest: an overview. Tree Physiol. 17:491–499.

Mitchell, J.F.B. 1983. The seasonal response of a general circulation model to changes in CO_2 and sea temperature. Q. J. R. Meteorol. Soc. 109:113–152.

Pastor, J., R.H. Gardner, V.H. Dale and W.M. Post. 1987. Successional changes in nitrogen availability as a potential factor contributing to spruce declines in boreal North America. Can. J. For. Res. 17:1394–1400.

Ryan, M.G., M.B. Lavigne and S.T. Gower. 1997. Annual carbon cost of autotrophic respiration in boreal forest ecosystems in relation to species and climate. J. Geophys. Res. (Atmos.) (D2). 102:28871–28883.

Saliendra, N.Z., J.S. Sperry and J.P. Comstock. 1995. Influence of leaf water status on stomatal response to humidity, hydraulic conductance, and soil drought in *Betula occidentalis*. Planta 82:1220–1229.

Sato, N., P.J. Sellers, D.A. Randall, E.K. Schneider, J. Shukla, J.L. Kinter, III, Y.T. Hou and E. Albertazzi. 1989. Effects of implementing the Simple Biosphere Model (SiB) in a general circulation model. J. Atmos. Sci. 46:2757–2782.

Saugier, B., A. Granier, J.-Y. Pontailler, E. Dufrêne and D.D. Baldocchi. 1997. Transpiration of a boreal pine forest measured by branch bags, sap flow and micrometeorological methods. Tree Physiol. 17:511–519.

Sellers, P.J., Y. Mintz, Y.C. Sud and A. Dalcher. 1986. A simple biosphere model (SiB) for use within general circulation models. J. Atmos. Sci. 43:505–531.

Sellers, P.J., J.A. Berry, G.J. Collatz, C.B. Field and F.G. Hall. 1992. Canopy reflectance, photosynthesis and transpiration. Part III: A reanalysis using improved leaf models and a new canopy integration scheme. Remote Sens. Environ. 42:187–216.

Sellers, P.J., F.G. Hall, H.A. Margolis, R. Kelly, D.D. Baldocchi, G.D. Hartog, J. Cihlar, M.G. Ryan, B. Goodison, P. Crill, K.J. Ranson, D. Lettenmaier and D.E. Wickland. 1995. The Boreal Ecosystem–Atmosphere Study (BOREAS): an overview and early results from the 1994 field year. Bull. Am. Meteorol. Soc. 76:1549–1577.

Sellers, P.J., L. Bounoua, G.J. Collatz, D.A. Randall, D.A. Dazlich, S. Los, J.A. Berry, I. Fung, C.J. Tucker, C.B. Field and T.G. Jensen. 1996*a*. A comparison of the radiative and physiological effects of doubled CO_2 on the global climate. Science 271:1402–1406.

Sellers, P.J., D.A. Randall, G.J. Collatz, J.A. Berry, C.B. Field, D.A. Dazlich, C. Zhang and G.D. Collelo. 1996*b*. A revised land surface parameterization (SiB2) for atmospheric GCMs. Part 1. Model formulation. J. Clim. 9:676–705.

Sellers, P.J., R.E. Dickinson, D.A. Randall, A.K. Betts, F.G. Hall, J.A. Berry, G.J. Collatz, A.S. Denning, H.A. Mooney, C.A. Nobre, N. Sato, C.B. Field and A. Henderson-Sellers. 1997. Modeling the exchanges of energy, water, and carbon between continents and the atmosphere. Science 275:502–509.

Sheriff, D.W., J.P. Mattay and R.E. McMurtrie. 1996. Modeling productivity and transpiration of *Pinus radiata*: climatic effects. Tree Physiol. 16:183–186.

Solomon, A.M. and T. Webb, III. 1985. Computer-aided reconstruction's of late-Quaternary landscape dynamics. Annu. Rev. Ecol. Syst. 16:63–84.

Sperry, J.S. 1995. Limitations on stem water transport and their consequences. *In* Plant Stems: Physiology and Functional Morphology. Ed. B.L. Gartner. Academic Press, San Diego, pp 105–124.

Sperry, J.S. and W.T. Pockman. 1993. Limitation of transpiration by hydraulic conductance and xylem cavitation in *Betula occidentalis*. Plant Cell Environ. 16:279–287.

Tans, P.P., I.Y. Fung and T. Takahashi. 1990. Observational constraints on the global atmospheric CO_2 budget. Science 247:1431–1438.

Tilman, D. 1987. Secondary succession and the pattern of plant dominance along experimental nitrogen gradients. Ecol. Monogr. 57:189–214.

Van Cleve, K. and J. Yarie. 1986. Interaction of temperature, moisture, and soil chemistry in controlling nutrient cycling and ecosystem development in the taiga of Alaska. Ecol. Stud. 57:160–169.

Van Cleve, K., L. Oliver, R. Schlenter, L.A. Viereck and C.T. Dyrness. 1983. Productivity and nutrient cycling in taiga forest ecosystems. Can. J. For. Res. 13:747–766.

von Caemmerer, S. and G.D. Farquhar. 1981. Some relationships between biochemistry of photosynthesis and the gas exchange of leaves. Planta 153:376–387.

Wullschleger, S.D. 1993. Biochemical limitations to carbon assimilation in C_3 plants—A retrospective analysis of the A/C_i curves from 109 species. J. Exp. Bot. 44:907–920.

Yoder, B.J., M.G. Ryan, R.H. Waring, A.W. Schoettle and M.R. Kaufmann. 1994. Evidence of reduced photosynthetic rates in old trees. For. Sci. 40:513–527.

Yue, D., Y. Desjardins, M. Lamarre and A. Gosselin. 1992. Photosynthesis and transpiration of *in vitro* cultured asparagus plantlets. Sci. Hortic. 49:9–14.